

MODELING ELECTRON EMISSION AND SURFACE EFFECTS FROM DIAMOND CATHODES*

D. A. Dimitrov, J. R. Cary, D. Smithe, C. Zhou, Tech-X Corp., Boulder, CO 80303, USA
 I. Ben-Zvi, T. Rao, J. Smedley, E. Wang, BNL, Upton, NY 11973, USA

Abstract

We developed modeling capabilities, within the Vorpal particle-in-cell code, for three-dimensional (3D) simulations of surface effects and electron emission from semiconductor photocathodes. They include calculation of emission probabilities using general, piece-wise continuous, space-time dependent surface potentials, effective mass and band bending field effects. We applied these models, in combination with previously implemented capabilities for modeling charge generation and transport in diamond, to investigate the emission dependence on applied electric field in the range from approximately 2 to 17 MV/m along the [100] direction. The simulation results were compared to experimental data when using different emission models, band bending effects, and surface-dependent electron affinity. Simulations using surface patches with different levels of hydrogenation lead to the closest agreement with the experimental data.

INTRODUCTION

High-average current and high-brightness electron beams are needed in advanced applications such as ultra-high Free-Electron Lasers, electron cooling of hadron accelerators, and Energy-Recovery Linac light sources. Semiconductor cathodes with negative electron affinity are known [1] to have good quantum efficiency (QE) (10% achieved experimentally) properties. To address the high brightness requirements for these applications, a new design for a photoinjector with a diamond amplifier was proposed [2] and is currently being investigated (see, e.g. [3–5] and references therein).

The operation of the diamond-amplifier cathode consists of using first a primary beam of electrons, accelerated to about 10 keV, (or photons with similar energies) to impact a diamond sample. The energetic primary electrons scatter inelastically generating secondary electrons. These electrons, and their related holes, relax their energies initially by producing more electron-hole pairs and later by scattering with phonons.

In applied electric field, the generated electrons and holes drift in opposite directions and are separated. The secondary electrons are transported towards a diamond surface with a negative electron affinity (NEA). Part of these electrons are then emitted into the accelerating cavity of an electron gun. The NEA is used to enhance the emission. Two orders of magnitude charge amplification (number of emitted electrons relative to the number of injected primary ones) has been observed in different experiments [4,5].

Investigation of the phenomena involved in using diamond for generation of amplified electron beams via simulations requires modeling of secondary electron generation, charge transport, and electron emission. We have now implemented models for these processes in the Vorpal computational framework [6,7].

MODELING ELECTRON EMISSION

The overall modeling approach involves three main steps shown in the simplified digram in Fig. 1. First, creation of (secondary) electrons in the conduction band and holes in the valence band is started by inelastic scattering with highly energetic primary electrons. Next, the free electrons and holes relax their energies via inelastic scattering (creating more electron-hole pairs and/or emission/absorption of phonons). Field is applied causing electrons to drift towards the band bending region (BBR) that ends with a (usually hydrogenated) negative electron affinity surface. In the final step, the electrons are emitted or reflected when they attempt to cross the diamond-vacuum interface.

For the secondary electron generation, we used our implementation of the Tanuma–Powell–Penn model. For modeling charge transport, we used a Monte Carlo approach. Detailed description of these modeling capabilities is provided in Ref. [6]. Recently, we implemented several emission mod-

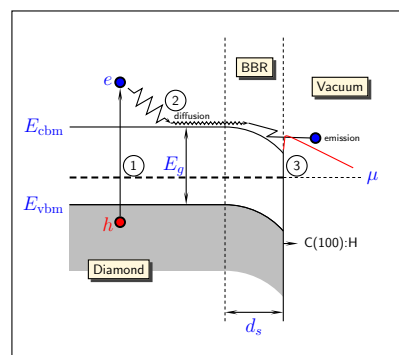


Figure 1: Three main processes are modeled: electron-hole generation, charge transport, and electron emission from surfaces with different potentials and band bending regions.

els and started using them to study electron emission from semiconductor cathodes [7] (and references therein for use of these models to investigate electron emission from GaAs). For the results presented here, we used our implementation of the transfer matrix (TM) model for calculation of emission probabilities and a surface potential energy that includes the effect of the image charge:

$$V(x) = \chi - Fx - Q/x, \quad (1)$$

* We are grateful to the U.S. DoE Office of Basic Energy Sciences for supporting this work under grants DE-SC0006246 and DE-SC0007577.

where χ is the electron affinity (EA) in eV, F is the applied external field (in eV/m), x is the distance from the emission surface, $Q = Q_0 (K_s - 1) / (K_s + 1)$ with K_s the static dielectric constant of the emitter ($K_s = 5.7$ for diamond), and Q_0 is a constant (in eV·m). The TM method allows us

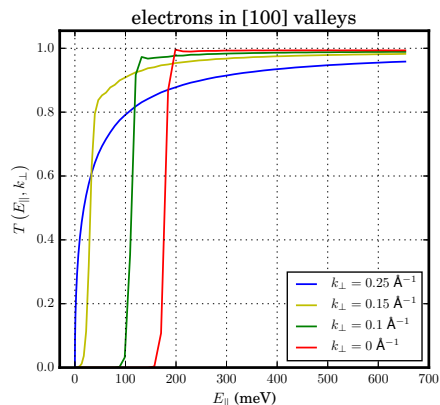


Figure 2: Emission probabilities calculated with the TM model directly include conservation of transverse momentum and electron mass anisotropy effects.

to directly include in the emission probability calculation the conservation of transverse electron momentum and the change of the electron mass from diamond to vacuum [7]. Conservation of transverse electron momentum is a particularly important effect for emission from diamond (100) surfaces. It allows direct emission only from two of the six equivalent conduction band valleys. Sample emission probabilities calculated from the TM model are shown in Fig. 2 as a function of electron normal (to the emission surface) energy for several transverse wavevectors. The electron affinity was set to $\chi = 0.3$ eV and the applied field to 15 MV/m.

RESULTS

We ran end-to-end three-dimensional (3D) simulations to investigate how surface properties included in the implemented models affect results on the probability of emission in comparison to available experimental data [4]. We also considered energy distribution properties of emitted electrons in relation to a different emission mechanism used to interpret experimental data from a hydrogenated surface of a boron-doped diamond [8].

We set up the simulations similarly to the approach developed in the transmission and emission mode experiments [4] used to deduce emission probability vs applied field from measured collected charge. By analogy with the experiments, we define a probability of emission from simulations data using the ratio:

$$P_{sim}(F) = N_{em}(F) / N_{tr}(F), \quad (2)$$

where $N_{em}(F)$ is the number of emitted electrons at the given external field magnitude F and $N_{tr}(F)$ is the number of electrons transported successfully to the emission surface. A typical simulation domain used had lengths of $8 \times 20 \times 20$

μm with the diamond region around $6.5 \mu\text{m}$ long and the vacuum around $1.5 \mu\text{m}$. Example charge transport and electron emission regimes are shown in Fig. 3. The potential of the electrostatic solver is set such that the holes (shown in blue on the left plot in Fig. 3) are collected on the left side and the electrons are transported to the emission surface. The right plot in

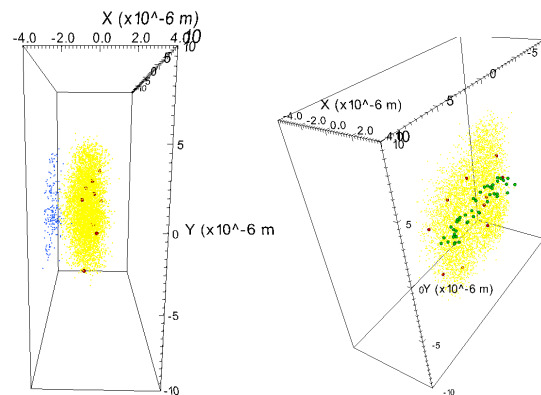


Figure 3: Visualization of particle evolution confirms expected charge amplification (left; primary electrons are in red and secondary ones in yellow) and electron emission from a diamond surface with non-uniform electron affinity (right; vacuum electrons are in green).

Fig. 3 shows the emitted electrons in green. The emission surface was set to have non-uniform electron affinity with a smaller value over a central stripe of given area relative to a higher value for the rest of the emission surface. This leads to electron emission mostly from the central stripe with the lower electron affinity as shown in in Fig. 3. Comparison of experimental data from four similarly prepared diamond samples [4] with results from simulations that include different surface effects and properties are shown in Fig. 4. The top plot in Fig. 4 shows results from runs with uniform EA. The EA χ and the (downward) band bending magnitude W are the only parameters varied in the simulations. The results show that we can find χ and W values that lead to qualitative agreement [7] with the experimental data. However, the probability vs field curves from the simulations have a different shape than the ones from the experiments.

As Fig. 4 indicates, the experimental data from the four different diamond samples (that were prepared in the same way) show variation in the measured probabilities. One way to interpret this variation is to consider that the hydrogenation was not uniform on the resulting emission surfaces. We explored this in the simulations by considering a central patch on the emission surface (with a given area as a fraction of the total emitting area) with a lower electron affinity relative to the rest of the emission surface that was at a higher electron affinity. Results from such simulations are shown in the bottom plot of Fig. 4. The central patch was at $\chi = 0.17$ eV and the rest of the surface at $\chi = 0.55$ eV. The area of the central patch was varied. The results from these simulations lead to improved agreement with the experimental data.

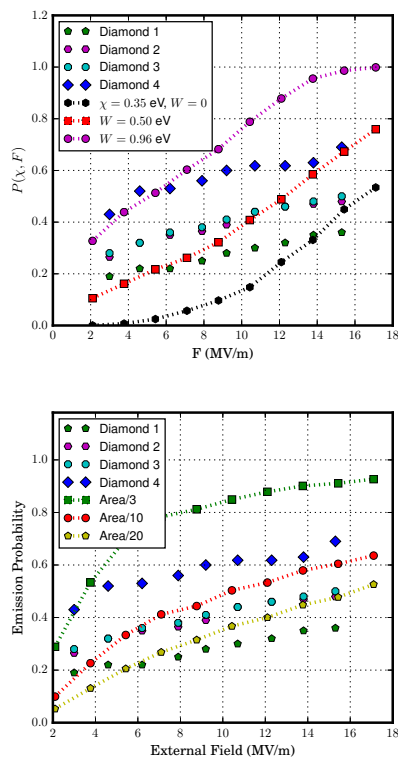


Figure 4: Comparison of emission probabilities from experiments with simulations using uniform electron affinity indicate qualitative agreement (top). Surfaces with non-uniform EA lead to better agreement (bottom).

Moreover, the observed curves now have a similar shape to the experimental ones.

Finally, we consider specific energy distribution properties of emitted electrons shown in Fig. 5. These plots indicate the number of electrons successfully emitted with the corresponding kinetic energies E they hit the diamond emission surface. The data is plotted vs the electron conserved transverse wavevector. The top row of plots is for an emission surface with uniform $\chi = 0.35$ eV in 5.43 MV/m external field. Top left plot is without band bending (BB). The top right is with downward BB magnitude of $W = 0.5$ eV. As expected, this leads to increase in electron emission. However, the mean transverse energy (MTE) of emitted electrons increases from $\langle E_{\perp} \rangle = 21.41$ meV without BB to 43.69 meV with BB. The bottom row of plots is from runs with non-uniform χ (data from the same runs as in Fig. 4 with the lower $\chi = 0.17$ eV central patch area fraction of 1/10). The bottom left plot is again with $F = 5.43$ MV/m. The data on the bottom right plot is from the run with $F = 13.77$ MV/m. It shows emission of electrons with lower energies due to the Schottky lowering of the surface barrier when increasing the applied field. The MTE was 23.66 meV for the run with $F = 5.43$ MV/m and 27.09 meV when $F = 13.77$ MV/m. The smaller change in MTE is due to electron emission mainly from the central patch with smaller electron affinity. The rest of the emission surface stops most of the transported electrons leading to charge accumulation there.

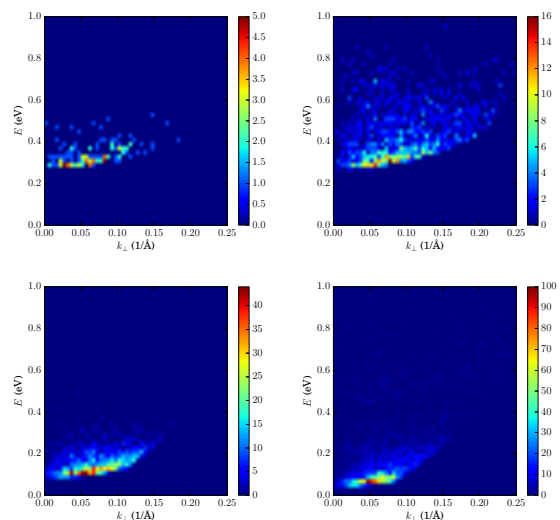


Figure 5: Electron impact energies of emitted electrons vs conserved transverse momentum (or $k_{\perp} = p_{\perp}/\hbar$) indicate how band bending and applied electric field affect the energy distribution of emitted electrons (see text for further details).

SUMMARY

We implemented end-to-end modeling of charge generation, transport, and electron emission from diamond. This allowed us to investigate emission from a (100) diamond surface with different electron affinity properties. Simulations with a non-uniform electron affinity surface showed the closest agreement with experimental data from high-purity diamond samples [4]. The implemented models, however, are not sufficient to describe the data from true negative electron affinity, high boron-doping diamond [8], apart from the main emission peak (0-0) reported since conservation of transverse momentum allows emission only from the conduction band valleys along the [100] axis. Including phonon-assisted electron emission processes in the modeling is needed to allow for emission from perpendicular valleys and for energies of emitted electrons corresponding to the satellite peaks reported by Rameau *et al.* [8].

REFERENCES

- [1] D. H. Dowell *et al.*, *Nucl. Instr. Meth. Phys. Res. A* **622**, 685, 2010.
- [2] I. Ben-Zvi *et al.*, C-AD Accel. Phys. Rep. C-A/AP/149, BNL, 2004.
- [3] X. Chang *et al.*, *Phys. Rev. Lett.* **105**, 164801, 2010.
- [4] E. Wang *et al.*, *Phys. Rev. ST Accel. Beams* **14**, 111301, 2011.
- [5] K. M. O'Donnell *et al.*, *Adv. Func. Mat.* **23**, 5608, 2013.
- [6] D. A. Dimitrov *et al.*, *J. Appl. Phys.* **108**, 073712, 2010.
- [7] D. A. Dimitrov *et al.*, *J. Appl. Phys.* **117**, 055708, 2015.
- [8] J. D. Rameau *et al.*, *Phys. Rev. Lett.* **106**, 137602, 2011.